Structural investigations of the xTeO-(1-x)GeO (x=0, 0.2, 0.4, 0.6, 0.8 and 1) tellurite glasses: A composition dependent Raman spectroscopic study

A.G. Kalampounias, N.K. Nasikas, G.N. Papatheodorou

Author's Accepted Manuscript

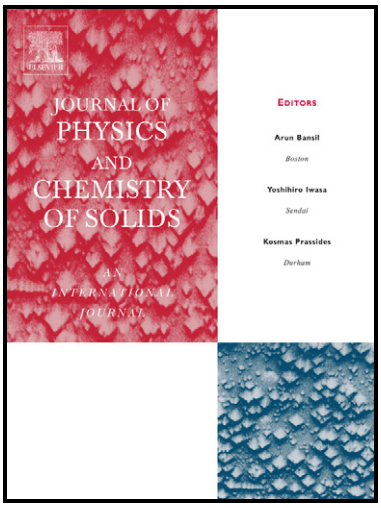

www.elsevier.com/locate/jpcs

Structural investigations of the $xTeO_2$-(1-x)GeO_2 (x = 0, 0.2, 0.4, 0.6, 0.8 and 1) tellurite glasses: A composition dependent Raman spectroscopic study

A.G. Kalampounias, N.K. Nasikas, G.N. Papatheodorou

PII: S0022-3697(11)00153-3
DOI: doi:10.1016/j.jpcs.2011.05.016
Reference: PCS 6473

To appear in: *Journal of Physics and Chemistry of Solids*

Received date: 19 October 2010
Revised date: 3 May 2011
Accepted date: 31 May 2011

Cite this article as: A.G. Kalampounias, N.K. Nasikas and G.N. Papatheodorou, Structural investigations of the $xTeO_2$-(1-x)GeO_2 (x = 0, 0.2, 0.4, 0.6, 0.8 and 1) tellurite glasses: A composition dependent Raman spectroscopic study, *Journal of Physics and Chemistry of Solids*, doi:10.1016/j.jpcs.2011.05.016

Submitted to J. Phys. Chem. Solids
October 19, 2010

Structural investigations of the $xTeO_2$-$(1-x)GeO_2$ (x = 0, 0.2, 0.4, 0.6, 0.8 and 1) tellurite glasses: A composition dependent Raman spectroscopic study

A. G. Kalampounias[1,2,*], N. K. Nasikas[1,3] and G. N. Papatheodorou,[1]

[1] *Foundation for Research and Technology Hellas – Institute of Chemical Engineering and High Temperature Chemical Processes, FORTH/ICE-HT, P.O. Box 1414, GR – 26 504, Patras, Greece*
[2] *Department of Chemical Engineering, University of Patras, GR – 26 504, Patras, Greece*
[3] *Department of Materials Science, University of Patras, GR – 26 504, Patras, Greece*

Abstract

Raman spectra of $xTeO_2$-$(1-x)GeO_2$ (x = 0, 0.2, 0.4, 0.6, 0.8 and 1) germanium tellurite glasses were measured and analyzed in an effort to follow the structural changes caused by mixing two typical glass-formers. Systematic Raman intensity measurements have been performed in an effort to elucidate the composition induced structural changes and a possible mechanism that accounting for these changes was proposed. The network structure of the glass is characterized by TeO_4 trigonal bipyramid mixed with TeO_3 trigonal pyramid units, while GeO_4 tetrahedral units are also present. Changing the GeO_2 content results to conversion of the TeO_4 units to TeO_3 units with a neutral doubly-bridged oxygen atom, while the existence of charged terminal oxygen atoms is questionable. The measured relative Raman intensities are semi quantitatively correlated to the transformation of the TeO_4 trigonal bipyramid into TeO_3 trigonal pyramids.

Keywords: A. amorphous materials, A. glasses, A. non-crystalline materials, A. oxides, C. Raman spectroscopy

* Corresponding author. Department of Chemical Engineering, University of Patras & Foundation for Research and Technology Hellas – Institute of Chemical Engineering and High Temperature Chemical Processes, P.O. Box 1414, GR–26504 Patras, Greece. Tel.: +30 2610 969 558; fax: +30 2610 997 849; e–mail: angelos@chemeng.upatras.gr

1. Introduction

Tellurite glasses have scientific and technological interest due to their attractive physical properties such as low melting points, high dielectric constant [1, 2], high refractive index [2] and good infrared transmissivity [3]. The refractive indices allow the utilization of these glasses for non-linear optical materials [4] and the phonon energies have at least two important consequences, the improved infrared transmission up to 6 μm and the low multiphonon decay rates compared to other network oxide glasses. Furthermore, tellurite glasses possess chemical durability and are water resistive [5].

Currently, there exist a large amount of literature regarding the structure of pure TeO_2 and xM_2O-$(1-x)TeO_2$ (M_2O: alkali oxide, x: mole fraction) glasses with a variety of techniques such as X-ray diffraction [6-8], neutron diffraction [8, 9], NMR [10-12], Mösbauer spectroscopy [13], EXAFS [14], ab initio quantum-mechanical calculations [15, 16], molecular orbital calculations [9], Brillouin [17], IR [18, 19] and Raman scattering [20-23]. However, a limited number of papers have been focused on binary glassy systems where both components are glass-formers participating directly in the formation of the vitreous network.

For the present work we have prepared the binary glasses $xTeO_2$-$(1-x)GeO_2$ (x = 0, 0.2, 0.4, 0.6, 0.8 and 1) and study them at room temperature by vibrational Raman spectroscopy. The data are discussed in terms of the glass structure, while emphasis has been given in the local environment around Te and Ge atoms and the effect of composition variation on the structure.

2. Experimental

The reagent grade chemicals Tellurium (IV) oxide (99.99% purity) and Germanium (IV) oxide (99.95% purity) were purchased from Alfa Aesar. The appropriate amounts of polycrystalline TeO_2 and glass powder GeO_2 were mixed and melted in platinum crucibles at 700-800^oC for 15-30 min. The homogenized bubble-free liquids were quenched using the conventional method by dipping the crucible into cold water. Heating of the samples was performed at temperatures near the glass transition temperature in order to avoid cracking due to relieve internal stresses generated by quenching.

Raman measurements were obtained using a high-resolution UV–Visible Labram HR-800 spectrograph (JY, ISAHoriba group) excited with the 441.8 nm line of an air-cooled HeCd laser of Kimmon Electric Co. (Dual, 325/442 nm, UV/blue, 20/80 mW; IK5651R-G model laser). All room temperature spectra were recorder in a backscattering geometry under a microscope where the excitation laser beam was focused onto the sample by a microscope objective (50×/0.55). Spectral slit widths (resolution) were set equal to 2 cm^{-1}, while the scattered light was detected by a CCD detector. Both polarized (VV: vertical polarization of incident laser – vertical analysis of scattered light) and depolarized (VH: vertical polarization of incident laser – horizontal analysis of scattered light) scattering geometries were employed for glasses. A calibration procedure with the aid of a CCl_4 sample was often taking place in order to check the polarization and correct for possible drifts of the monochromator's gratings. Accumulation times were adjusted to result in a very high signal-to-noise ratio.

3. Results and Discussion

Room temperature polarized (VV) and depolarized (VH) Raman spectra were measured for germanium tellurite glasses $xTeO_2$-$(1-x)GeO_2$ with x = 0, 0.2, 0.4, 0.6, 0.8 and 1. The spectra of the "end "glasses and their polarization characteristics were found to be the same as reported before [24, 25]. Fig. 1 shows the polarized Raman spectra of the systems studied in the reduced representation. The benefits of using the reduced representation in analyzing the spectra has been discussed elsewhere [26]. Systematic and gradual intensity and frequency changes of the main bands are observed with composition indicating continuous and overlapping structural modifications of the participating glass formers.

Gaussian analysis of the spectra was performed using the nonlinear regression method based on the Levenberg–Marquardt algorithm. The major component bands correspond to unresolved peak maxima and slope changes in the experimental polarized and depolarized spectra in all fits. This constrains the minimum number of major component bands, their positions and widths, thus involving only few free fitting parameters. A representative example of the deconvolution procedure is shown in the bottom of Fig. 1, where the complete fit of the pure TeO_2 spectrum is shown. Four Gaussian profiles are shown in the high-frequency spectral envelop (500-850 cm^{-1}) of TeO_2 glass. These bands are approximately located at 769, 715, 644 and 583 cm^{-1} and are marked as D, C, B and A, respectively. In the medium frequency range [400 – 500 cm^{-1}] one Gaussian profile, located at 457 cm^{-1}, can be resolved under the broad spectral envelop of the glass. Below 400 cm^{-1}, a set of at least three broad bands at ~353, ~294 and ~162 cm^{-1} is required to fit the glass spectra.

It has been proposed that the TeO_2 glass is mainly composed of TeO_4 trigonal bipyramid units (tbp) and of TeO_3 trigonal pyramid units (tp) (see Fig. 2(a) and 2(b)). In TeO_4 (tbp) units,

one equatorial site of the sp^3d hybrid orbitals is occupied by a lone pair of electrons and the other two equatorial and axial sites are occupied by oxygen atoms. In TeO_3 (tp) units, one of the Te sp^3 hybrid orbitals is occupied by a lone pair of electrons [27]. Ab initio molecular orbital calculations have shown that the stretching motion of the doubly bonded oxygen in the $TeO_{2/2}$=O tp unit is expected at ~868 cm^{-1} [16]. In the tbp units, most of the tellurium atoms are connected at vertices by Te – $_{equatorial}$ O_{axial} – Te, linkage, which connects two distinct tbp units, having the oxygen atom in equatorial (short bond distance) for the first and in axial site (long bond distance) for the second tbp unit, respectively [28]. Thus, TeO_2 glass has a unique structure owing to these units and its connecting style considerable differs from the conventional glass formers, such as B_2O_3, SiO_2, GeO_2 and P_2O_5. This would infer that TeO_2 may have a structural role differing than that of other conventional oxides in binary glasses which contain network modifiers. Many authors have proposed, based on Raman spectroscopic results, that the primary structural unit of tellurite glasses having high TeO_2 content is a distorted TeO_4 tbp and that the fraction of TeO_3 trigonal pyramids (tp) increases with increasing mono- or di-valent cation oxide content and/or temperature (see e.g. :[20-23])

The origin of the main bands appearing in the reduced polarized (VV) Raman spectrum of TeO_2 glass according to the deconvolution process (bottom of Fig. 3) are tentatively assigned as follows. The bands at ~769 (D) and ~715 cm^{-1} (C) have been assigned to stretching modes of TeO_3 tp units. The doublet at ~644 (B) and ~583 cm^{-1} (A) has been assigned to the stretching modes of the TeO_4 tbp units. The two different peaks are presumably related to the two non-equivalent oxygen atoms (those at the equatorial plane and those out of the plane). Further, the broad peak at ~457 is assigned to Te – O – Te and/or O – Te – O linkages [20, 21]. The existence of this band indicates the presence of a continuous network consisting of vertex-sharing

tellurium – oxygen polyhedra. The peaks observed at below 330 cm^{-1} in the low-frequency region are assigned to a bending vibration of TeO_3 tp having or not charged terminal oxygen atoms [20, 21]

With increasing the GeO_2 content, the 457 cm^{-1} band of tellurite network merges with the 420 cm^{-1} band of pure GeO_2, which is assigned to the symmetric stretching of bridging oxygen atoms (Ge-O-Ge) in 6-membered GeO_4 rings [25, 29]. The ~347 and ~520 cm^{-1} bands in the GeO_2 rich spectra are attributed to D_1 and D_2 defect modes, respectively. The former band is related to Ge 'deformation' motion within the network, while the latter is related to breathing motion of bridging oxygen atoms in 3-membered GeO_4 rings [25, 29]. In the 500-620 cm^{-1} region of pure GeO_2 and GeO_2 rich compositions, the Ge-O-Ge bending modes are present as shoulder bands at ~556 and 595 cm^{-1}. These bands are assigned to TO and LO split modes associated with significant Ge and O motion, respectively. The high-frequency bands observed at ~860 and 998 cm^{-1} are the TO and LO split asymmetric stretching bands of the bridging oxygen atoms (Ge-O-Ge) [29]. The TO mode possibly coexists with the expected stretching motion of the doubly bonded oxygen in the $TeO_{2/2}$=O tp unit at ~868 cm^{-1} from ab initio molecular orbital calculations [16]. Due to the strong overlapping of the above reported bands, the population of the doubly bonded oxygen in the $TeO_{2/2}$=O tp units cannot be estimated directly from the Raman data**.**

The deconvolution results of the high-frequency Raman spectra for all compositions are shown in Fig. 3. Apart from the four bands (A - D) attributed to TeO_3 tp and TeO_4 tbp units, three other bands have been deconvoluted in the higher frequency region of the spectra. These bands are assigned to the asymmetric stretching region of the $v_3(F)$ tetrahedral mode of GeO_2 in analogy to the pure SiO_2 spectrum [30]. Three component modes are expected in the low-

symmetry distortion fields and indeed three can be resolved in our spectra, which exhibit the same polarization characteristics. Increasing GeO_2 content cause an intensification of the Raman peaks in the range 700–790 cm^{-1} at the expense of the peaks located at lower frequencies implying a gradual transformation from TeO_4 tbp to TeO_3 tp units. In parallel, a continuous intensity increase of the high-frequency bands appears revealing a strengthening of the germanate network. Furthermore, the frequencies of the A to D bands exhibit an almost linear increase as shown in Fig. 3. The observed blue shift in the frequencies of the peaks attributed to TeO_4 tbp and TeO_3 tp structural units is probably due to the substitution of Te atoms in the tellurite network by Ge atoms with increasing the amount of GeO_2 content in the binary system. The substitution of Te atoms by Ge atoms, which possess almost half atomic weight, reduce the "effective mass" leading in tern to blue shift in the vibrational frequencies of the TeO_4 tbp and TeO_3 tp structural units. The assignment of the blue shift in the Raman spectra to new or mixed structural species is questionable.

In an effort to quantitatively follow the local structure transformation of the TeO_4 units into TeO_3 units directly from the spectroscopic data, a new procedure was proposed [31]. In this procedure it was assumed that the reduced Raman intensity ratio, $r = (I_{red}^{VV}(C) + I_{red}^{VV}(D))/(I_{red}^{VV}(A) + I_{red}^{VV}(B))$ is proportional to the mole fraction or concentration ratio of R=["TeO_3"]/["TeO_4"], then the systematics of the structural changes occurring can be examined on the basis of the relation between R and composition variation. In view of the lack of any other information, we tacitly assume here that the Raman cross-sections of the symmetric stretching modes of these two units are comparable. Figure 5 shows the intensity ratio of the deconvoluted Raman peaks versus GeO_2 content. There is an almost linear dependence of the

intensity ratio on the composition. These results suggest that the conversion of the TeO_4 tbp units to TeO_3 tp units is enhanced by increasing the Ge/Te ratio on the glass matrix.

Since the present glasses are formed by two network formers, it is expected that, unlike alkali tellurite glasses, a few $Te\text{-}O^-$ and $Ge\text{-}O^-$ charged terminal bonds exist in GeO_2-TeO_2 glasses. No vibrations due to charged $Te\text{-}O^-$ and $Ge\text{-}O^-$ bonds are observed in the Raman spectra of these glasses. In alkali tellurite glasses, charged $Te\text{-}O^-$ stretching vibration is observed in the frequency range 700-800 cm^{-1} [27a], while for charged $Ge\text{-}O^-$ these vibrations appear above 1000 cm^{-1} [29]. These vibrations are missing in our spectra. With increasing the GeO_2 content, a decrease of the intensities of A and B bands accompanied by a parallel increase of the C and D bands takes place (Fig.1). Bands A and B are related to the fraction of Te atoms forming TeO_4 tbp's, while C and D bands correspond to Te atoms forming TeO_3 tp units. This suggests that a part of TeO_4 tbp polyhedra change into TeO_3 tp units with increasing the GeO_2 content. In alkali tellurite glasses the conversion of TeO_4 to TeO_3 is induced by the addition of high basicity oxygen accompanied with alkali oxide or alkaline earth oxide, which act as network modifiers The GeO_2 is a known representative glass former but, it seems that in the case of GeO_2-TeO_2 glasses the GeO_2 acts like a network modifier that causes cleavage of Te-O-Te linkages and steps up the conversion of TeO_4 to TeO_3 units. Such conversion is presumably less effective in comparison with the TeO_4 to TeO_3 conversion caused by the alkali tellurite network modifiers.

A schematic representation of the overall structure is shown in Fig. 2 (c), where GeO_4 tetrahedral units are interconnected via common oxygen atoms to trigonal bipyramidal and trigonal pyramidal units. The amount of TeO_3 (tp) units depends on the GeO_2 content. The stretching Te-O frequency of trigonal bipyramidal $TeO_{3/2}O^-$ and trigonal pyramidal $TeO_{1/2}O^- = O$ units with charged terminal bonds is expected to appear in the 800-1000 cm^{-1}

frequency range. The absence of these bands in our spectra even for high GeO_2 content indicates that the presence of such species is questionable.

4. Conclusions

In this paper we present a detailed analysis of the Raman spectra of $xTeO_2$-$(1-x)GeO_2$ (x = 0, 0.2, 0.4, 0.6, 0.8 and 1) germanium tellurite glasses over a broad composition range aiming in elucidation of the structural changes caused by mixing two typical glass-formers. The network structure of the glass is formed by mixing TeO_4 trigonal bipyramid and TeO_3 trigonal pyramid units. GeO_4 tetrahedral units are also present, while the presence of mixed polyhedra is questionable. With increasing the GeO_2 content, a gradual conversion of the TeO_4 units to TeO_3 units with a neutral doubly-bridged oxygen atom takes place with a parallel increase of their vibrational frequencies. No spectral evidence appears for the presence of charged terminal oxygen atoms in the network. Detailed analysis of the reduced Raman spectra made it possible to quantitatively follow the transformation of the TeO_4 trigonal bipyramids—that dominates in the TeO_2 rich glasses—into TeO_3 trigonal pyramids with composition variation and a structural model accounting for the tellurite network was proposed.

References

[1] D. R. Ulrich, J. Am. Ceram. Soc. 47 (1964) 595.

[2] J. E. Stanworth, Nature 169 (1952) 581.

[3] H. Burger, W. Vogel, V. Kozhukharov, Infrared Phys. 25 (1985) 395.

[4] K. Shioya, T. Kmatsu, H. G. Kim, R. Sato, K. Matsusita, J. Non-Cryst. Solids 189 (1995) 16.

[5] M. J. Redman, J. H. Chen, J. Am. Ceram. Soc. 50 (1967) 523.

[6] G. W. Brady, J. Chem. Phys. 27 (1) (1957) 300.

[7] Y. Dimitriev, J. C. J. Bart, V. Dimitrov, M. Z. Arnaudov, Z. Anorg. Allg. Chem. 479 (1981) 229.

[8] J. C. McLaughlin, S. L. Tagg, J. W. Zwanziger, J. Phys. Chem. B, 105 (2001) 67.

[9] H. Niida, T. Uchino, J. Jin, S.-H. Kim, T. Fukunaga, T. Yoko, J. Chem. Phys. 114 (1) (2001) 459.

[10] S. Sakida, S. Hayakawa, T. Yoko. J. Non-Cryst. Solids 243 (1999) 1.

[11] S. Sakida, S. Hayakawa, T. Yoko. J. Non-Cryst. Solids 243 (1999) 13.

[12] J. C. McLaughlin, S. L. Tagg, J. W. Zwanziger, D. R. Haeffner, S. D. Shastri, J. Non-Cryst. Solids 274 (2000) 1.

[13] T. Nishida, M. Yamada, H. Ide, Y. Ikushima, J. Mater. Sci. 25 (1990) 3546.

[14] A. Osaka, Q. Jianrong, T. Nanba, J. Takada, Y. Miura, T. Yao, J. Non-Cryst. Solids 142 (1992) 81.

[15] O. Noguera, M. Smirnov, A. P. Mirgorodsky, T. Merle-Mejean, P. Thomas, J.-C. Champarnaud-Mesjard, J. Non-Cryst. Solids 345-346 (2004) 734.

[16] T. Uchino, T. Yoko, J. Non-Cryst. Solids 204 (1996) 243.

[17] M. Ahart, T. Yagi, Y. Takagi, Physica B, 219-20 (1996) 550.[18] N. Mochida, K. Takahashi, K. Nakata, S. Shibusawa, J. Ceram. Soc. Jpn, 86 (7) (1978) 316.

[19] M. Dimitrova-Patkova, Y. Dimitriev, M. Arnaudov, V. Dimitrov, Phys. Chem. Glasses 30 (6) (1989) 260.

[20] T. Sekiya, N. Mochida, A. Ohtsuka, M. Tonokawa, J. Non-Cryst. Solids 144 (1992) 128.

[21] M. Tatsumisago, T. Minami, Y. Kowada, H. Adashi, Phys. Chem. Glasses 35 (2) (1994) 89; A. G. Kalampounias, G. N. Papatheodorou, S. N. Yannopoulos, J. Phys. Chem. Solids, 67 (2006) 725.

[22] M. Tatsumisago, S.-K. Lee, T. Minami, Y. Kowada, J. Non-Cryst. Solids 177 (1994) 154; A. G. Kalampounias, S. N. Yannopoulos, G. N. Papatheodorou, J. Phys. Chem. Solids, 68 (2007) 1035.

[23] O. Noguera, T. Merle-Mejean, A. P. Mirgorodsky, M. B. Smirov, P. Thomas, J.-C. Champarnaud-Mesjard, J. Non-Cryst. Solids 330 (2003) 50; A. P. Mirgorodsky, T. Merle-Mejean, J.-C. Champarnaud, P. Thomas, B. Frit, J. Phys. Chem. Solids 61 (2000) 501.

[24] T. Sekiya, N. Mochida, A. Ohtsuka, M. Tonokawa, J. Ceram. Soc. Jpn. Inter. Ed. 97 (1989) 1440.

[25] F. L. Galeener, J. Non-Cryst. Solids, 40 (1980) 527.

[26] G. N. Papatheodorou and S. N. Yannopoulos, in *Molten Salts:From Fundamentals to Applications*, edited by M. Gaune-Escard (Kluwer Academic, Dordrecht, 2002), pp. 47–106.

[27] T. Sekiya, N. Mochida, A. Ohtsuka, M. Tonokawa, J. Non-Cryst. Solids 144 **(**1992) 128; M. Tatsumisago, T. Minami, Y. Kowada, H. Adashi, Phys. Chem. Glasses 35 **(**1994) 89;

O. Noguera, T. Merle-Mejean, A. P. Mirgorodsky, M. B. Smirov, P. Thomas, J-C Champarnaud-Mesjard, J. Non-Cryst. Solids 330 (2003) 50.

[28] T. Sekiya, N. Mochida, A. Ohtsuka, M. Tonokawa, J. Ceram. Soc. Jpn. 97 (1989) 1440.

[29] L. Giacomazzi, P. Umari, A. Pasquarello, Phys. Rev. Lett., 95 (2005) 075505; G. S. Henderson, G. M. Bancroft, M. E. Fleet, D. J. Rogers, Am. Minerals, 70 (1985) 946; G. S. Henderson, M. E. Fleet, J. Non-Cryst. Solids, 134 (1991) 259; M. Micoulaut, L. Cormier, G. S. Henderson, J. Phys.: Condens. Matter 18 (2006) R753.

[30] A. G. Kalampounias, S. N. Yannopoulos, G. N. Papatheodorou, J. Chem. Phys., 124 (2006) 014504.

[31] A. G. Kalampounias, G. N. Papatheodorou, S. N. Yannopoulos, J. Phys. Chem. Solids, 68 (2007) 1029.

Figure captions

Fig. 1

Reduced polarized (VV) Raman spectra of $xTeO_2$-(1-x)GeO_2 (x = 0, 0.2, 0.4, 0.6, 0.8 and 1) glasses at room temperature. Fitting example is shown only for pure TeO_2 glass. Open circles: experimental data (only 33 % of the experimental points are shown for clarity). Thick solid line: total fit curve. Gaussian lines: individual vibrational peaks. The various components are described in the text.

Fig. 2

Schematic model of the structure of $xTeO_2$-(1-x)GeO_2 glasses. The addition of GeO_2 into the $TeO_{4/2}$ network leads to the formation of TeO_3 tp with neutral terminal bonds ($TeO_{2/2}$=O). The basic structural unit in the binary tellurite glasses is the TeO_4 tbp in TeO_2-rich glasses, while $GeO_{4/2}$ tetrahedral units are present with increasing the amount of GeO_2.

Notation: tbp=trigonal bipyramids and tp=trigonal pyramid.

Fig. 3

Deconvoluted polarized (VV) Raman spectra of $xTeO_2$-(1-x)GeO_2 (x = 0, 0.2, 0.4, 0.6, 0.8 and 1) glasses at room temperature. Open circles: experimental data (only 33 % of the experimental points are shown for clarity). Thick solid lines: total fit curve. Gaussian lines: individual vibrational peaks.

Fig. 4

Compositional dependence of the frequencies of deconvoluted peaks observed in polarized (VV) Raman spectra of $xTeO_2$-(1-x)GeO_2 (x = 0, 0.2, 0.4, 0.6, 0.8 and 1) glasses at room temperature.

Fig. 5

Stretching modes intensity ratio $r = (I_{red}^{VV}(C) + I_{red}^{VV}(D))/(I_{red}^{VV}(A) + I_{red}^{VV}(B))$ vs GeO_2 content at ambient temperature. Line is drown as guide to the eye. See text for details concerning the deconvolution procedure.

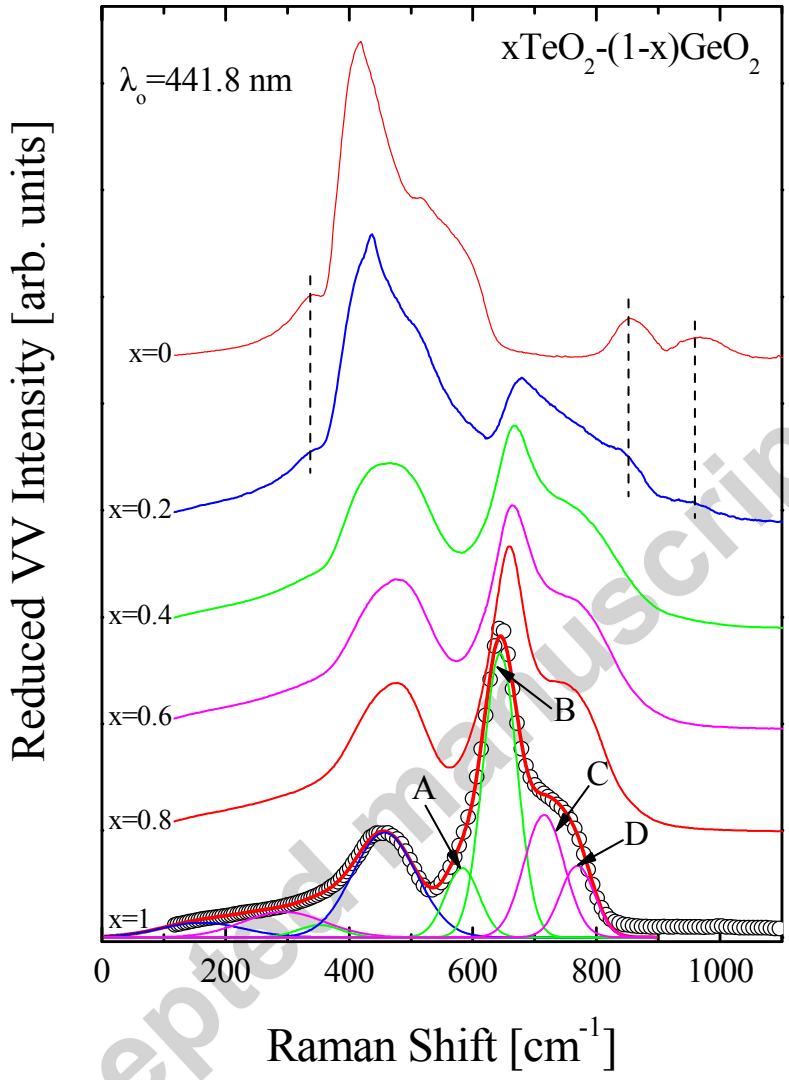

Figure 1

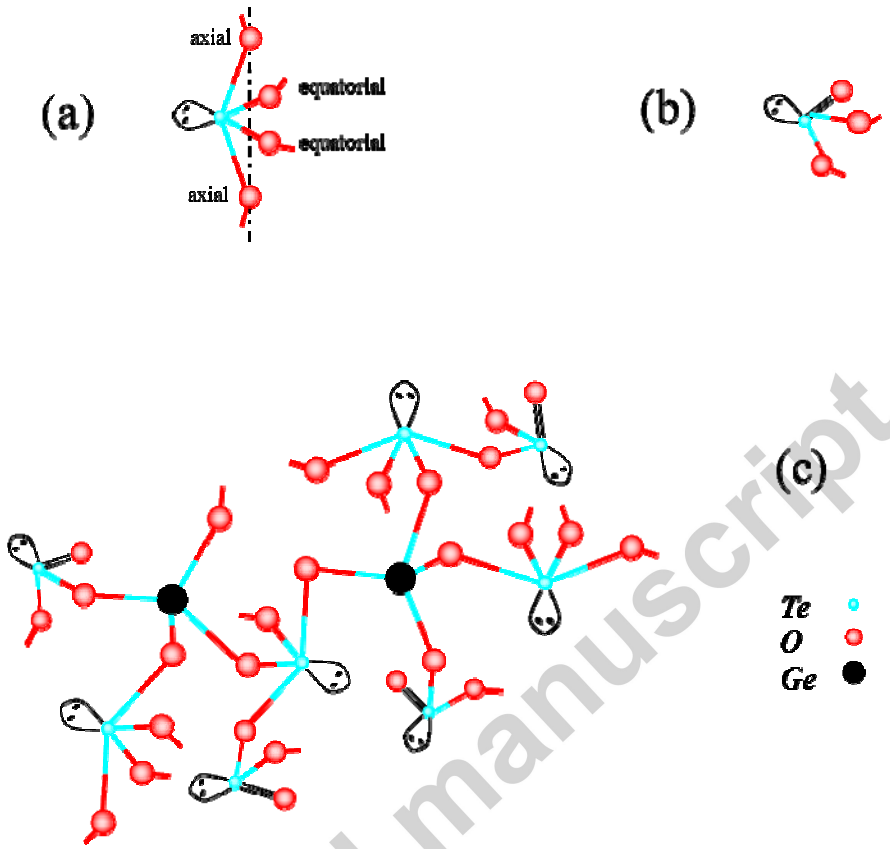

Figure 2

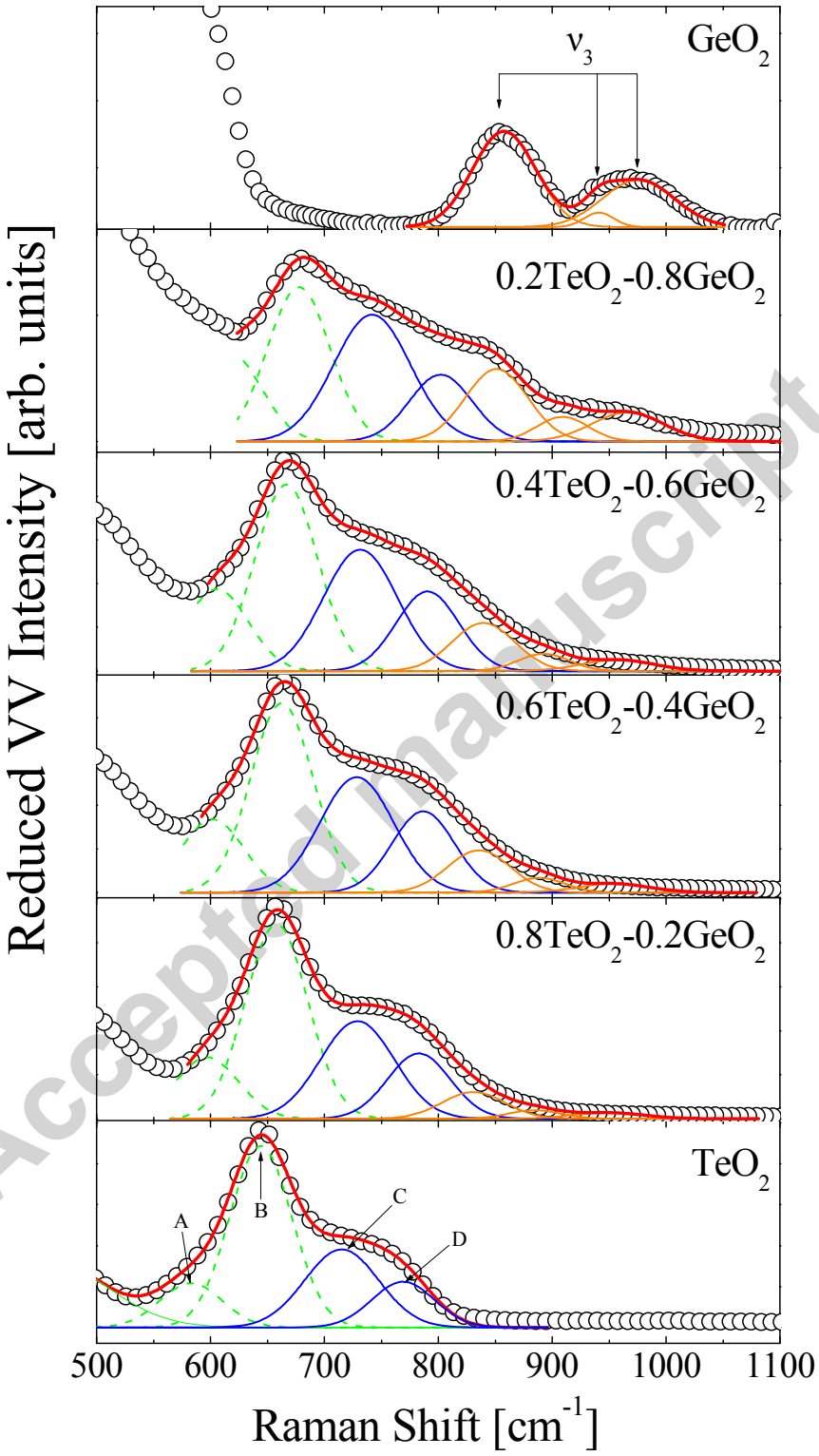

Figure 3

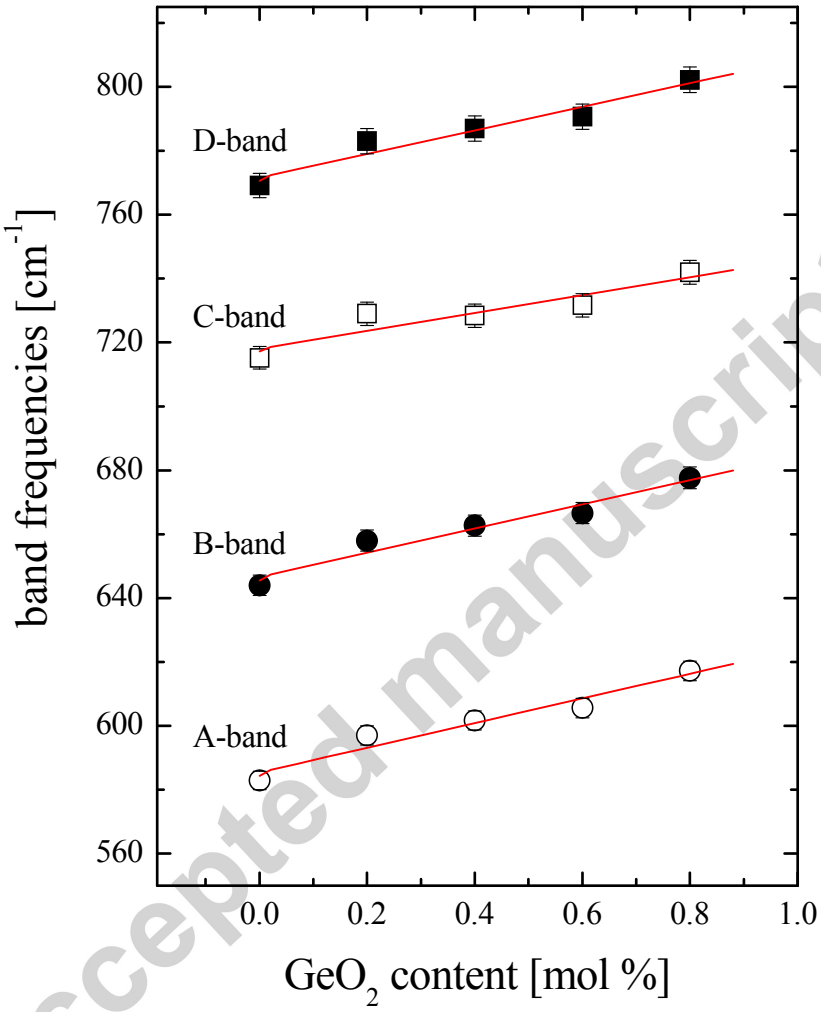

Figure 4

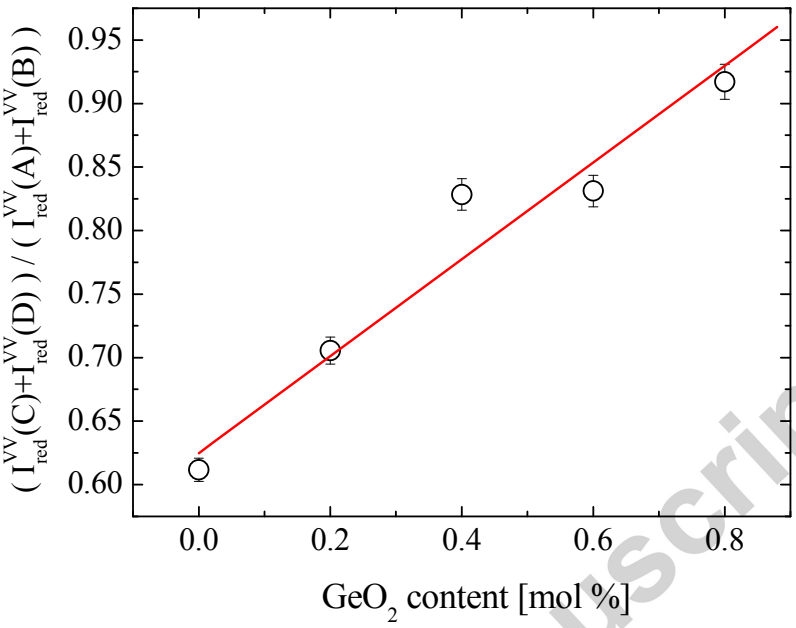

Figure 5

- Study of binary glasses with both components participating in the vitreous network formation
- Emphasis has been given in the Te and Ge local environment and the composition effect on the structure
- Quantitative estimation of the TeO_4 tbp into TeO_3 tp transformation with composition variation
- A structural model accounting for the tellurite network is proposed
- Correlation between glass stability and structural alterations